Iranian Journal of Astronomy and Astrophysics
Vol. 11, No. 3, Summer 2024, 177–191
©Available online at http://ijaa.du.ac.ir
DOI: 10.22128/ijaa.2024.846.1185
Online ISSN: 2383–403X

Iranian Journal of Astronomy and Astrophysics

Research Paper

Chameleon Screening and Fifth Force in Globular Clusters I: King Model

Mohadese Mousavi*[1] · Mohammad Taghi Mirtorabi[2] · Tahereh Azizi[3]

[1] Department of Theoretical Physics, Faculty of Basic Sciences, University of Mazandaran, P. O. Box 47416–95447, Babolsar, Iran;
*email: s.mousavi02@umail.umz.ac.ir

[2] Department of Fundamental Physics, Faculty of Physics, Alzahra University, Tehran, Iran;
email: torabi@alzahra.ac.ir

[3] Department of Theoretical Physics, Faculty of Basic Sciences, University of Mazandaran, P. O. Box 47416–95447, Babolsar, Iran;
email: t.azizi@umz.ac.ir

Received: 1 July 2024; **Accepted:** 4 December 2024; **Published:** 28 December 2024

Abstract. Those globular clusters that are located in the halo of galaxy experience a weak gravitational force due to their great distance from the center of their host galaxy, so they are characterized by extremely low gravitational potential. This unique characteristics make them important subjects of research in various fields. The study of clusters, analyzing the dynamics and gravitational interactions within them, offers a unique opportunity to explore the implications of modified gravity theories, such as fifth force interactions or unscreened regions. In our paper, we explore the presence and extent of an unscreened region in the outer layers of an isothermal sphere, as represented by the King model and influenced by a chameleon field. Also, we consider the acceleration resulting from the chameleon field and then, proceed to calculate the line-of-sight velocity dispersion under the influence of the chameleon and compare it with Newtonian predictions. Our findings reveal that the dynamical impact of the fifth force can be observed throughout the entire of the globular cluster.

Keywords: Modified gravity, Screening mechanism, Chameleon theory, King profile

1 Introduction

Einstein's theory of general relativity (GR) is regarded as one of the most significant scientific accomplishments of the last century [1]. It provides a comprehensive explanation of space-time, gravity, and matter, resulting in a new perception of the universe. This theory has been verified in many experiments, with one of the most significant being the solar system tests [2]. While general relativity has been remarkably successful in describing gravity, there are still some issues and limitations, such as GR does not imply that it is valid on all scales in any environment. The discrepancy between theoretical predictions and observations on cosmic scales, such as the distribution of galaxies, and the cosmic microwave background radiation, indicates the existence of dark matter, and the discovery of accelerated cosmic expansion demonstrates the need for dark energy. Therefore, various gravity models have

* *Corresponding author*

been proposed. These alternative gravitational models are attempting to explain these contradictions without the need to assume the existence of dark matter and dark energy, are typically referred to as modified gravity (MOG), where the Einstein-Hilbert action is modified and revised, see [3–6] and references therein.

There are several theoretical models of modified gravity, which are classified in different ways. One category of models involves adding an extra degree of freedom, such as scalar, vector, or tensor fields to the metric. In general, modified gravity theories admit a modified Poisson's equation in weak field approximation and then an extra force called fifth force. So, modified gravity theories' primary challenge is passing the Solar System tests, where have not revealed any sign of such extra force to overcome this discrepancy. The screening mechanism is recommended as a crucial tool for the influence of the fifth force to be greatly diminished or even completely eliminated in dense environments [4,5]. Screening methods can be classified according to their capacity to suppress the influence of the fifth force on a spherical object, and one method is thin-shell screening. Thin-shell screening mechanisms are a group of theories that include chameleon [7,8], Symmetron [9], and Dilaton [10] screening. Each mechanism operates differently, but they all involve the creation of a thin shell around an object that screens its gravitational effects [11]. In chameleon mechanism the local density of a place determines the mass of a field. According to Yukawa's theory, fields with greater mass have shorter force ranges. Thus, the field has a higher mass in dense areas, resulting in an extremely short range for this force [12].

Astrophysical objects, such as stars, clusters, and galaxies provide excellent laboratories for exploring the need for modified gravity theories. We review a summary of the researches that has been done in this particular field: The application of thin-shell screening in the study of main-sequence stars and galaxies has shown that unscreened stars can have significantly higher luminosity and shorter lifetimes [13]. This finding has implications for dwarf galaxies, as unscreened stars within them could potentially increase the total galactic luminosity. Additionally, the authors of ref. [14] used the MOG theory of Moffat for eight dwarf spheroidal galaxies of the Milky Way for testing modified gravity. In this context, the thin-shell screening mechanism, [15] has used a modified version of Modules for Experiments in Stellar Astrophysics (MESA) to study the structure of Red Giant Branch (RGB) stars. This investigation examines how the chameleon process operates within a star and how they provide constraints on modified gravity. The findings suggest that RGB stars with a screened core and unscreened mantle are denser and, as a result, have higher temperatures compared to normal Newtonian stars in the standard regime. In the same context, [16] specifically investigated stellar and gaseous rotation curves based on chameleon theory in dwarf galaxies. Additionally, in [17], the study considers the chameleon and symmetron screening mechanisms and utilizes data from the Alfalfa HI survey to examine observable displacement between stars and gas in galaxies. The operation of the chameleon mechanism within inhomogeneous RGB stars was investigated by [18]. Furthermore, the chameleon mechanism was investigated in inhomogeneous astrophysical objects [19]. Another work done in this field is related to the chameleon field around a radially pulsating mass [20]. The wide range of astrophysical experiments in the field of screened modified gravity was done by [21–26].

Among the celestial bodies, we consider globular clusters. They experience minimal external field effects from the host galaxy on their dynamics, due to their large distance from the galaxy's center. This results in a weak gravitational potential, which means that screening does not occur within them. As a result, the effects of the fifth force can be observed, making them suitable laboratories for testing modified gravity. Another reason for choosing globular clusters is the availability of several theoretical models that explain their dynamics. This means that there is various information available about their systems that can be tested, including density, velocity dispersion, and more. As a result, several authors ([27–33]) have investigated Modified Newtonian Dynamics and MOG in globular clusters. In this context, Moffat's modified gravity theory enabled him to determine the velocity dispersion of various globular clusters and then compare the results with observational data [34]. Investigating modified gravity in globular clusters, focusing on NGC 2419 as a case study based on the symmetron theory found that the presence of a scalar field can increase the velocity at the center of the globular cluster, ultimately improved the fit between theoretical and observed velocity dispersion [35].

In this paper, we propose the idea of how the screening mechanism in the modified theory of gravity can affect globular clusters. To achieve this, we should initiate by checking theoretical models that formally are being used to explain the dynamics of stellar clusters. Here, our main focus is to detect any observable unscreened region that a chameleon field can induce on the surface of a King profile as a model of the spherical system. Based on this, we can theoretically obtain measurable quantities such as the line of sight velocity dispersion and compare these values with the Newtonian predictions. In future studies, we can compare these theoretical values with observations of specific globular clusters.

The paper is structured as follows: Section 2 provides a brief overview of the concept of the King model. Section 3 outlines the chameleon modified gravity. In section 4, we examine the unscreened area in globular clusters in chameleon gravity. Finally, we present the findings and conclusions in sections 5.

2 The King model

A common method for interpreting the behavior of a star cluster is through the use of theoretical models based on a distribution function, denoted by $f(\vec{r}, \vec{v}, t)$. This function represents the average number of stars in the phase-space volume around a given position $\vec{r}$ and velocity $\vec{v}$ [36]. The dynamical evolution of the cluster is described by the collision-less Boltzmann equation, which can be expressed as

$$\vec{v}.\nabla_r f - \nabla_r \Phi.\nabla_v f = 0\,, \tag{1}$$

where Φ is the smoothed gravitational potential. Jean's theorem states that any function of the motion's constants has the potential to be a solution to the equation (1). This allows for the development of various models by selecting the constant of motion. As a result, different models can be created depending on the chosen constant of motion. When dealing with spherical systems, the distribution function is dependent on the energy per unit mass. The isothermal sphere is a basic model that is commonly used for these systems; however, it is not a realistic model due to its infinite density at a large radius. To address this issue, a more realistic model known as the King model was introduced. This model utilizes a modified distribution function and is considered a better alternative to the isothermal sphere [36,37].

The distribution function in the King model is represented as

$$f(\varepsilon) = \begin{cases} \rho_1 (2\pi\sigma^2)^{-3/2} (e^{\varepsilon/\sigma^2} - 1), & \text{if } \varepsilon > 0, \\ 0, & \text{if } \varepsilon \leq 0, \end{cases} \tag{2}$$

where σ is the velocity dispersion and $\varepsilon = \Psi - \frac{1}{2}v^2$ represents the relative energy, where $\Psi = -\Phi + \Phi_0$ is relative potential. King's model comprises several features and processes that are crucial for the system's dynamics. For simplicity, assume that all components have equal masses, and the velocity distribution is isotropic. In addition to dynamical equilibrium, tidal radiation occurs at a finite radius. Therefore, it is a suitable theoretical model that can be compared to observational data. The density is given by $\rho = \int f d^3v$ and it can be obtained as

$$\rho_K(\psi) = \frac{4\pi\rho_1}{(2\pi\sigma^2)^{3/2}} \int_0^{\sqrt{2\psi}} dv v^2 [exp(\frac{\Psi - \frac{1}{2}v^2}{\sigma^2}) - 1] \,. \tag{3}$$

Note that the density in terms of the radius is obtained by solving Poisson's equation

$$\bigtriangledown^2 \Psi = -4\pi G\rho.$$

Rewriting Poisson's equation by substituting equation (3) in terms of the dimensionless quantity $x \equiv \frac{r}{r_0}$ and defining $W \equiv \frac{\Psi}{\sigma^2}$, where r_0 is the King radius, we get

$$\frac{d^2W}{dx^2} + \frac{2}{x}\frac{dW}{dx} = -9\frac{\rho}{\rho_0} \,. \tag{4}$$

It is worth noting that the various values of W_0 result in different values of $\frac{\rho}{\rho_0}$ with respect to x. To locate the unscreened area within globular clusters, it is essential to utilize the density function. Based on the previously provided information, the Kings model appears to be the most appropriate option.

3 Chameleon modified gravity

In modified gravity classification, the introduction of additional degrees of freedom, such as scalar fields, gives rise to scalar-tensor theories that modify the Einstein-Hilbert action as

$$S = \int d^4x\sqrt{-g}\left\{\frac{M_{Pl}^2}{2}\mathrm{R} - \frac{1}{2}\nabla_\mu\phi\nabla^\mu\phi - V(\phi)\right\} + S_m[\tilde{g}_{\mu\nu}, \phi] \,, \tag{5}$$

where M_{Pl} represents the Planck mass, R is the Ricci scalar, g is the determinant of the metric, $\psi_m^{(i)}$ are matter fields, and ϕ is scalar field with a potential $V(\phi)$ which conformally coupled to matter through the Jordan frame metric $\tilde{g}_{\mu\nu}$. In this frame, the interaction between matter and the scalar field is not direct, and there is minimal coupling between matter and gravity. Particles continue to follow the geodesic of the Jordan frame metric, so the geodesic equation remains unmodified. However, the gravitational potential is modified, leading to the emergence of a fifth force. To better understand the dynamics of a scalar field and to simplify calculations, it is more appropriate to use the Einstein frame, which is connected to the Jordan frame through the use of a coupling function $A(\phi)$,

$$\tilde{g}_{\mu\nu} = A^2(\phi) g_{\mu\nu} \,. \tag{6}$$

In the Einstein frame, the interaction between matter and a scalar field through the effective metric results in the energy-momentum tensor not being conserved. This non-conservation leads to additional terms in the geodesic equation, which is commonly referred to as the *fifth force* [38]

$$F_i^\phi \equiv -(\frac{1}{A}\frac{\partial A}{\partial \phi})\partial^i \phi \,. \tag{7}$$

Up to now, detection of the fifth force has not been confirmed, so it should be screened. Various methods can be used to screen this force. One of these is a scalar field with a modified mass that operates within the range of interaction, which is the mechanism of chameleon theory.

3.1 Chameleon mechanism

The chameleon mechanism was proposed by [7,8]. To comprehend the operation of the chameleon screening mechanism, consider the following action in the Einstein frame

$$S = \int d^4x\sqrt{-g}\left\{\frac{M_{Pl}^2}{2}\mathrm{R} - \frac{1}{2}\partial\phi^2 - V(\phi)\right\} + S_m[A^2(\phi)g_{\mu\nu}, \psi_m]\,. \tag{8}$$

The coupling of a chameleon scalar field to a matter field through a conformal factor, $A(\phi)$. The equation of motion for the chameleon is derived by taking the variation of the action (8) is given by

$$\nabla^2\phi = V_{,\phi} - \frac{1}{A}\frac{\partial A}{\partial\phi}T_m\,. \tag{9}$$

Consider an exponential form for the conformal factor,

$$A(\phi) = e^{\frac{\beta\phi}{M_{pl}}}\,, \tag{10}$$

where β represents a dimensionless coupling constant. In the context of non-relativistic matter, the quantity T_m represents the trace of the energy-momentum tensor and serves as a measure of the matter density, $T_m \approx -\rho_m$. However, in the Einstein frame, this matter density is not conserved, so we need the definition of a new density using a conformal factor as following

$$A(\phi)\rho = \rho_m^{(E)}\,. \tag{11}$$

Consequently, the equation of motion becomes

$$\nabla^2\phi = V_{,\phi} + \frac{\partial A}{\partial\phi}\rho\,. \tag{12}$$

The equation of motion reveals that the scalar field is influenced not only by the potential $V(\phi)$, but also by the density of the matter field. The effective potential is a result of combining these two items as follows

$$V_{eff}(\phi) \equiv V(\phi) + \rho A(\phi)\,. \tag{13}$$

If we choose a runaway form for potential

$$V(\phi) = \frac{M^{4+n}}{\phi^n}\,, \tag{14}$$

where M is constant with unit mass and n is a positive constant, the first term of the effective potential continuously decreases, while the second term is an increasing function, so the effective potential has a minimum. To find the scalar field that gives a minimum of effective potential, one should solve

$$\frac{\partial V_{eff}}{\partial\phi}\,|_{\phi_{min}} = -n\frac{M^{4+n}}{\phi_{(min)}^{n+1}} + \rho\frac{\beta}{M_{pl}}e^{\frac{\beta\phi_{(min)}}{M_{pl}}} = 0\,, \tag{15}$$

$$\phi_{min} = \left[\frac{nM^{4+n}M_{pl}}{\rho\beta e^{\beta\phi_{min}/M_{pl}}}\right]^{1/n+1}\,, \tag{16}$$

and a mass of small fluctuation about minimum is

$$\begin{aligned} m^2_{min} &= \frac{\partial^2 V_{eff}}{\partial \phi^2} \mid_{\phi_{min}} \\ &= V_{,\phi\phi}(\phi_{min}) + \rho \frac{\partial^2 A(\phi_{min})}{\partial \phi^2} \\ &= \frac{n(n+1)M^{4+n}}{\phi(min)^{n+2}} + \frac{\beta^2}{M^2_{pl}} \rho e^{\frac{\beta\phi(min)}{M_{pl}}} . \end{aligned} \tag{17}$$

The minimum value of a scalar field and its mass depend on the local density, as described by equations (16) and (17). In a dense environment, a scalar field with a large mass will suppress the effect of the chameleon field, known as the screening mechanism. However, in areas with low matter density, the chameleon field can exhibit its effects. Consequently, certain parameters may be modified within the unscreened ranges.

3.1.1 Compact object

In order to evaluate the chameleon's performance within a compact object, we make the assumption that the object is static, has spherical symmetry with a radius of R_c, and has a homogeneous density ρ_c with a total mass $M_c = \frac{4}{3}\pi R_c^3 \rho_c$. So, the equation of motion becomes

$$\frac{d^2\phi}{dr^2} + \frac{2}{r}\frac{d\phi}{dr} = V_{,\phi} + \frac{\beta}{M_{pl}} \rho(r) e^{\beta\phi/M_{pl}} , \tag{18}$$

where

$$\rho(r) = \begin{cases} \rho_c, & \text{for } r < R_c, \\ \rho_{BG}, & \text{for } r > R_c, \end{cases} \tag{19}$$

There are two different solutions depending on the size of the object, whether it is large or small. Based on the astrophysical objects being considered, it is appropriate to use a solution for large objects. If the object is sufficiently large, the chameleon field can minimize its effective potential over most of the radius of the object. As a result, the field will only vary near the surface of the object, leaving a field gradient in a very thin shell near the surface. The thin shell starts from a specific radius known as the screening radius. Before this radius, the region is screened, meaning there is no fifth force present, and beyond the screening radius up to the edge of the object the region is unscreened. So, we divide up the object into three regions, a screened center, an unscreened shell, and an unscreened exterior. We assume $\beta\phi/M_{pl} \ll 1$, thus equation of motion (18) reduces to

$$\frac{d^2\phi}{dr^2} + \frac{2}{r}\frac{d\phi}{dr} = V_{,\phi} + \frac{\beta}{M_{pl}} \rho(r). \tag{20}$$

In the region $r < r_{scr}$, at $r = 0$ the effective potential is in its minimum state. So, the equation (20) becomes

$$\nabla^2 \phi \approx 0. \tag{21}$$

The field remains at its approximately constant value in the screen region, $\phi \approx \phi_c$, and starts to change around the screening radius. Near the screening radius, $r \approx r_{scr}$, the scalar field began to roll. In this state, $V_{,\phi} \ll \frac{\beta\rho}{M_{pl}} e^{\beta\phi/M_{pl}}$, also assumed $\frac{\beta\phi}{M_{pl}} \ll 1$. Thus the equation of motions in $r_{scr} < r < R_c$ becomes

$$\frac{d^2\phi}{dr^2} + \frac{2}{r}\frac{d\phi}{dr} \approx \frac{\beta}{M_{pl}} \rho_c. \tag{22}$$

The background density beyond the object is very low, so the equation of motion is obtained approximately

$$\frac{d^2\phi}{dr^2} + \frac{2}{r}\frac{d\phi}{dr} \approx 0. \tag{23}$$

By solving the equations of motion for the three mentioned regions and applying the boundary conditions ($\frac{\mathrm{d}\phi}{\mathrm{d}r} = 0$ at $r = 0.$ and $\phi \to \phi_*$ as $r \to \infty$), we can determine the field in each region

$$\begin{cases} \phi(r) \approx \phi_c, & 0 < r < r_{scr}, \\ \phi(r) = \frac{\beta\rho_c}{3M_{pl}}\left(\frac{r^2}{2} + \frac{r_{scr}^3}{r}\right) - \frac{\beta\rho_c r_{scr}^2}{2M_{pl}} + \phi_c, & r_{scr} < r < R_c, \\ \phi(r) \approx -\left(\frac{\beta}{4\pi M_{pl}}\right)\left(\frac{3\Delta R_c}{R_c}\right)\frac{M_c e^{-m_*(r-R_c)}}{r} + \phi_*, & r > R_c, \end{cases} \tag{24}$$

where r is the distance from the center of a compact object and

$$\frac{\Delta R_c}{R_c} = \frac{R_c - r_{scr}}{R_c} = \frac{\phi_* - \phi_c}{6\beta M_{pl}\Psi_c}, \tag{25}$$

where $\Psi_c = GM_c/R_c$ is the Newtonian potential. To determine the screening radius for each compact object, we can compare the field and its derivative in the unscreened region with those outside the object at $r = r_{scr}$.

4 Unscreened region in the king model

Our analysis aims to identify the unscreened areas in globular clusters, where the potential effects of MOG may be detected. Globular clusters were chosen as the subject of our study due to their location far from the center of their host galaxy, which makes them unaffected by the galaxy's gravity and an ideal laboratory for modified gravity experimentation [35]. One of the methods used to determine the screening radius is presented in [15]'s paper, where the screening radius is obtained by the following equation

$$\frac{GQ(R_c)}{R_c} + \int_{r_{scr}}^{R_c} \frac{GQ(r)}{r^2} \approx \varphi_*\,, \tag{26}$$

where, G is the gravitational constant, $Q(r)$ is defined as $8\alpha\pi \int_{r_{scr}}^{r} \rho(r')r'^2 dr$, α denotes a scalar coupling, ρ is the density function, R_c is the globular cluster radius, and φ_* represents the scalar field value at cosmic mean density.

The determination of the screening radius relies on the values of α and φ_*, which are predicted by chameleon theory. We make use of the approximate values presented in [15]. For the density distribution of globular clusters, we use the King model [37], which is one of the most common theoretical models that fit with spherical systems.

The screening radius is obtained by numerically solving the equation (26). To simplify the process, it is recommended to use dimensionless radii and density. This can be achieved by rescaling the radius as a fraction of r_0, where $x = \frac{r}{r_0}$. The King radius is defined as

$$r_0 = \sqrt{\frac{9\sigma_0^2}{4\pi G\rho_0}},$$

where σ_0 represents the velocity dispersion. Additionally, it is necessary to rescale the density with respect to the central density, $\zeta = \frac{\rho}{\rho_0}$, where ρ_0 is obtained from equation (3).

Ultimately, the equation (26) can be written as

$$\frac{\int_{x_{scr}}^{R_c/r_0}\zeta x^2 dx}{R_c/r_0} + \int_{x_{scr}}^{R_c/r_0} \frac{\int_{x_{scr}}^{x}\zeta x^2 dx}{x^2} dx \approx \frac{\varphi_*}{8\alpha\pi G}\frac{1}{\rho_0 r_0^2}\,. \tag{27}$$

Using the dimensionless King density profile, we solve equation (27) to resolve the unscreened regions in globular clusters across a range of W_0 values [39]. The width of the unscreened area, in terms of the king radius for various values of W_0, is shown in Figure 1, and each one is shown separately in Figure 3. In addition, table 1 displays the screen radius values

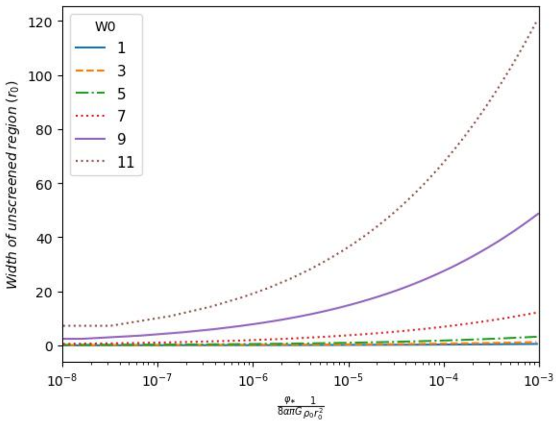

Figure 1: The width of the unscreened region according to the values of $\frac{\varphi_*}{8\alpha\pi G}\frac{1}{\rho_0 r_0^2}$. The width of the unscreened region, which displays the area that is considered from the edge of the cluster, is obtained in terms of r_0. So by considering an appropriate value for $\frac{\varphi_*}{8\alpha\pi G}\frac{1}{\rho_0 r_0^2}$, we can have the corresponding the width of the unscreened region.

for three different values of equation (27)'s right-hand side and different values of W_0s.

Table 1: The screening radius can be calculated by examining the King profile and comparing various values of $\frac{\varphi_*}{8\alpha\pi G}\frac{1}{\rho_0 r_0^2}$, across a range of W_0 values.

Screening radius (r_0)			
W_0 \ $\frac{\varphi_*}{8\alpha\pi G}\frac{1}{\rho_0 r_0^2}$	10^{-6}	10^{-7}	10^{-8}
1	1.83	1.91	1.94
3	4.37	4.54	4.62
5	9.75	10.23	10.45
7	29.86	31.60	32.65
9	115.22	121.96	125.47
11	314.67	331.57	342.14

Due to the presence of the fifth force in the unscreened area, both scalar and gravitational forces are exerted, resulting in a change in acceleration. As a result, acceleration will be applied differently for distances less than or greater than the screening radius (r_{scr}), as noted by [15].

$$\begin{cases} g_{eff} = -\frac{G(M(r)+\alpha Q(r))}{r^2}, & \text{for } r > r_{scr}, \\ g_{eff} = -\frac{GM(r)}{r^2}, & \text{for } r < r_{scr}. \end{cases} \tag{28}$$

Now, we can calculate the line of sight (LOS) velocity dispersion profile of globular clusters under the chameleon theory. The velocity dispersion in a spherically symmetric system can be determined using Jean's equation [36] as

$$\frac{\partial(\nu\sigma^2)}{\partial r} + \nu\frac{\partial\Phi}{\partial r} = 0\,, \tag{29}$$

where ν is the number density function, r is the radial distance from the center of the globular cluster, and Φ is the gravitational potential. Hence, the velocity dispersion can be obtained by the following equation

$$\sigma^2(r) = \frac{1}{\nu}\int_r^\infty \nu a(r^{'})dr^{'}\,, \tag{30}$$

where $a(r) = \frac{\partial\Phi}{\partial r}$. On the other hand, in observation, the line of sight velocity dispersion with respect to projected distance R is measured as

$$\sigma^2_{LOS}(R) = \frac{\int_R^\infty \frac{r\sigma^2(r)\nu(r)}{\sqrt{r^2-R^2}}dr}{\int_R^\infty \frac{r\nu(r)}{\sqrt{r^2-R^2}}dr}\,. \tag{31}$$

To calculate the line-of-sight velocity dispersion using MOG based on Chameleon, a specific quantity of $\frac{\varphi_*}{8\alpha\pi G}\frac{1}{\rho_0 r_0^2} \approx 10^{-6}$ is utilized to determine the screening radius. The equation (31) is then solved using numerical methods and the results are presented in Figure 2. We will compare the LOS-velocity dispersion of Newtonian gravity and MOG, as shown in Figure 4.

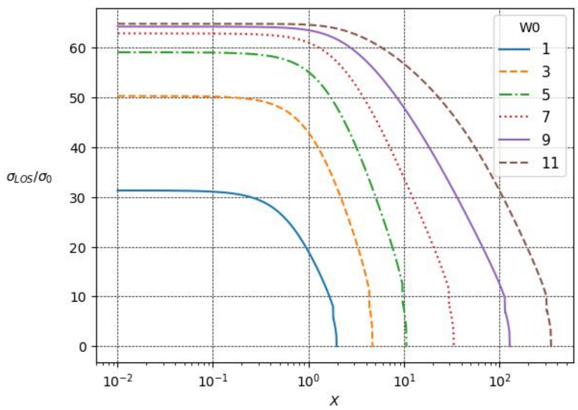

Figure 2: The predicted ratio of line of sight velocity dispersion of globular clusters to velocity dispersion in terms of dimensionless projected distance, where $X = R/r_0$, using the King model and Modified gravity based on Chameleon. The condition for finding the screening radius considers 10^{-6}.

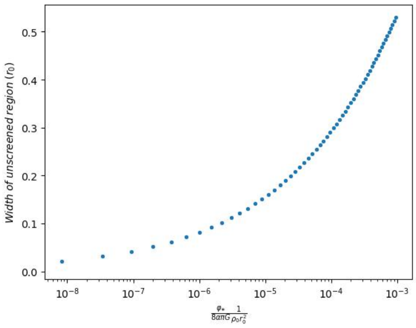

(a) W0 = 1

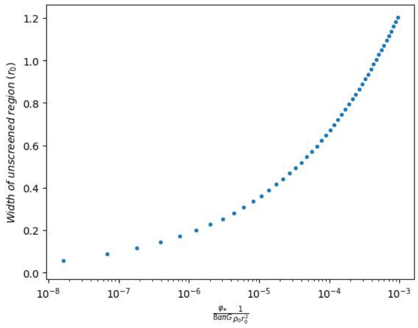

(b) W0 = 3

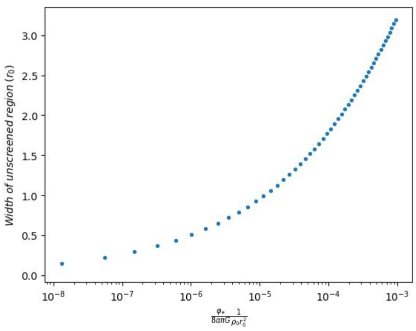

(c) W0 = 5

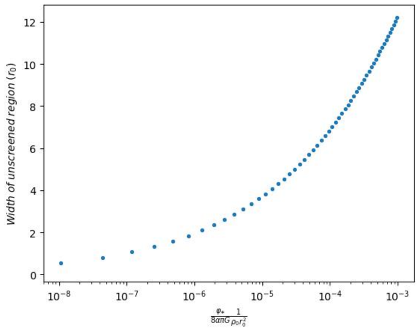

(d) W0 = 7

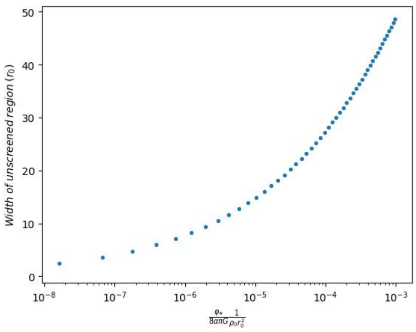

(e) W0 = 9

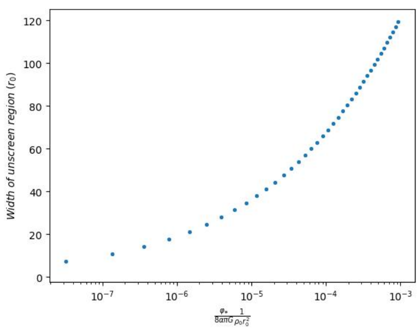

(f) W0 = 11

Figure 3: The chameleon theory for globular clusters predicts that the width of an unscreened region varies for each of the six values of W_0. The unscreened area differs depending on the value of $\frac{\varphi_*}{8\alpha\pi G}\frac{1}{\rho_0 r_0^2}$.

5 Conclusion

Numerous attempts have been made to describe the accelerated expansion of the universe following the discovery of cosmological acceleration. One approach that has been explored is the use of modified gravity models. However, these models have a notable drawback as they do not successfully pass tests conducted within the solar system. To address this issue, a screening mechanism can be employed to restore the validity of general relativity on the scale of the solar system. Scalar-tensor theories commonly employ the chameleon as a

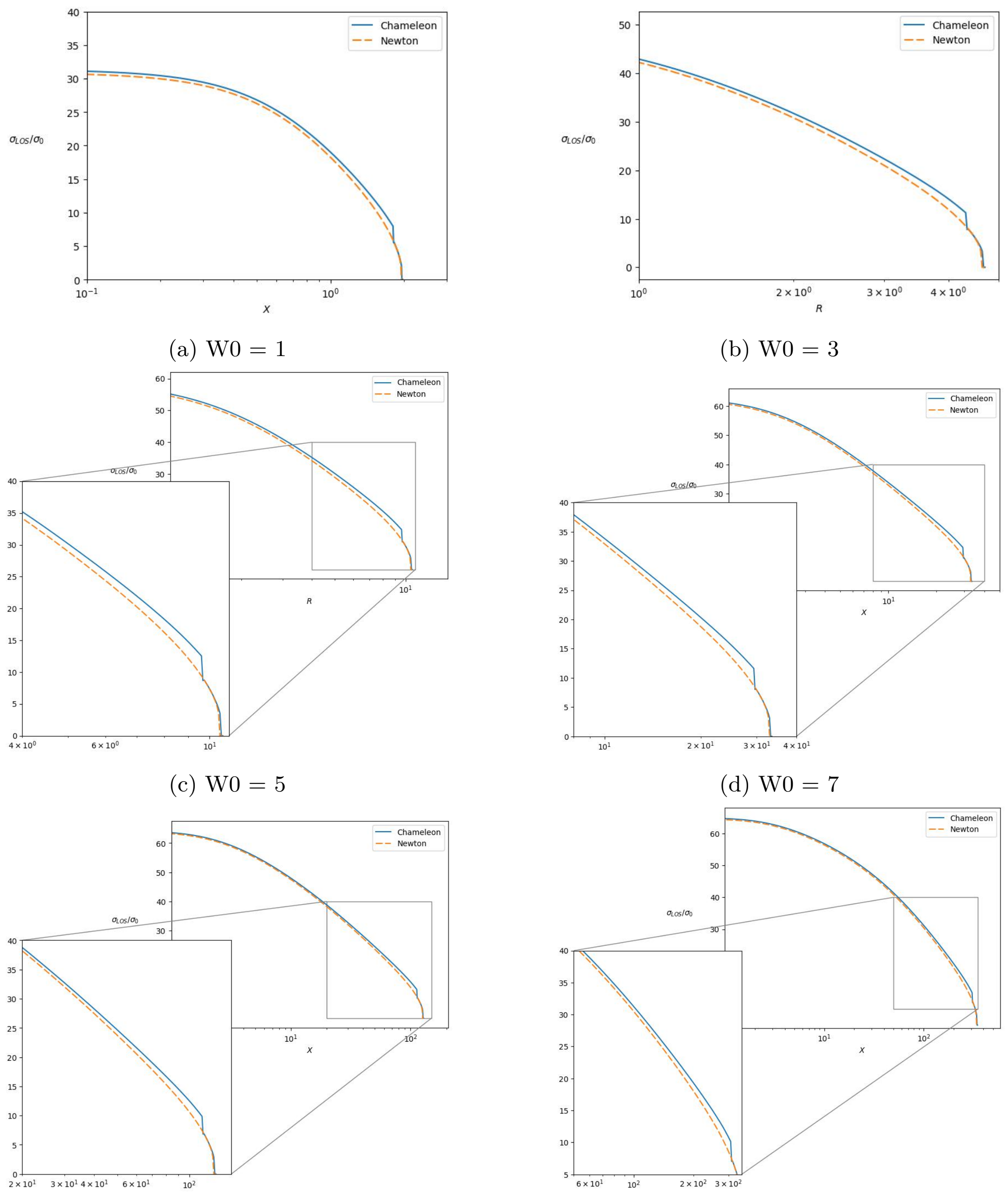

(a) W0 = 1
(b) W0 = 3
(c) W0 = 5
(d) W0 = 7
(e) W0 = 9
(f) W0 = 11

Figure 4: Los-velocity dispersion in MOG theory based on chameleon and Newtonian gravity for globular clusters. The results obtained for $\frac{\varphi_*}{8\alpha\pi G}\frac{1}{\rho_0 r_0^2} \approx 10^{-6}$. An attempt has been made to show the difference between two states.

screening mechanism that relies on local density. Regions with low density are considered ”unscreened”, where the scalar force from the chameleon field remains unobstructed. Researchers aim to observe a distinct effect of modified gravity in nature, particularly the force

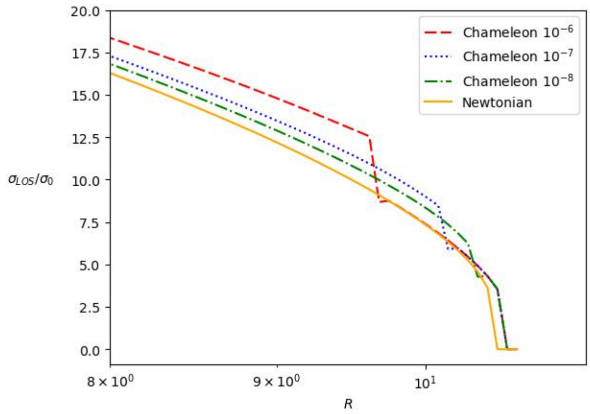

Figure 5: calculating los-velocity dispersion in MOG theory based on chameleon and standard gravity for globular clusters. To make a comparison, for $W_0 = 5$ three different values 10^{-6}, 10^{-7}, and 10^{-8} will be used for $\frac{\varphi_*}{8\alpha\pi G}\frac{1}{\rho_0 r_0^2}$.

resulting from the scalar field, known as the fifth force. One common method used to test modified gravity is by studying the impact of this fifth force on the structure and dynamics of globular clusters, which are spherically symmetrical systems with isotropic velocity dispersion. These star clusters are located at a considerable distance from the central region of their host, rendering them less susceptible to the gravitational potential exerted by the galaxy. This characteristic makes them particularly valuable for the study of modified gravity. When analyzing a star cluster, it is crucial to employ a dynamical model that can be readily compared to observational data. In this regard, the King models have gained a high reputation among observers as a basic model. To test modified gravity in globular clusters, we employed scalar-tensor modified gravity based on the screening mechanism. This allows us to investigate the presence of unscreened regions in globular clusters. The width of the unscreened region in terms of the King radius for various values of W_0 is determined by using the quantity of $\frac{\varphi_*}{8\alpha\pi G}\frac{1}{\rho_0 r_0^2}$, shown in Figure 1. As the ratio of $\frac{\varphi_*}{8\alpha\pi G}\frac{1}{\rho_0 r_0^2}$ decreases, the cluster's screening radius shifts towards the outer edge, resulting in a lower probability of finding the unscreened area. This result is illustrated in table 1. As we can see the difference between the obtained values for $\frac{\sigma_{LOS}}{\sigma_0}$ using three different values of $\frac{\varphi_*}{8\alpha\pi G}\frac{1}{\rho_0 r_0^2}$ and comparing them with the Newtonian value in the Figure 5 for $W_0 = 5$.

The velocity dispersion of globular clusters is a parameter with an available observational value. Linares had previously determined the line-of-sight velocity dispersion of the specific globular cluster based on the symmetron MG model [35]. Now, we are calculating the numerical line-of-sight velocity dispersion of globular clusters by fitting the King distribution function and using the chameleon theory. Ultimately, we will compare these results with the predictions of Newtonian gravity. Referring to the data presented in Figure 4, we have used a value of $\frac{\varphi_*}{8\alpha\pi G}\frac{1}{\rho_0 r_0^2} \approx 10^{-6}$ based on data from [15], to compare the line-of-sight velocity dispersion between chameleon modified gravity and Newtonian gravity for various values of $W_0 = 1, 3, 5, 7, 9, 11$. At this point, we observe that the values of the modified gravity model are slightly higher compared to those of the Newtonian mode. As a significant result, we found that LOS-velocity profile across the cluster disk could be affected by unscreened regions everywhere in the disc. As shown in Figure 4 the difference between Newtonian gravity and MOG is observable in an entire disc.

One method for assessing whether modified gravity is a better fit than Newtonian gravity is to compare the velocity dispersion of globular clusters obtained from both approaches with the observed values. This can be achieved by increasing the number of data points through future observations. This approach has the potential to detect modified gravity effects within clusters, which could provide evidence for the need for correction.

Acknowledgment

We are grateful to Hosein Haghi for his helpful discussions and guidance throughout the study.

Authors' Contributions

All authors have the same contribution.

Data Availability

The data that support the findings of this study are available from the corresponding author upon reasonable request.

Conflicts of Interest

The authors declare no potential conflicts of interest.

Ethical Considerations

The authors have diligently addressed ethical concerns, such as informed consent, plagiarism, data fabrication, misconduct, falsification, double publication, redundancy, submission, and other related matters.

Funding

This research did not receive any grant from funding agencies in the public, commercial, or nonprofit sectors.

References

[1] Einstein, A. 1916, Annalen Phys., 49, 769.

[2] Will, C. M. 2014, Living reviews in relativity, 17, 1.

[3] Clifton, T., Ferreira, P. G., Padilla, A., & Skordis, C. 2012, Physics reports, 513, 1.

[4] Joyce, A., Jain, B., Khoury, J., & Trodden, M. 2015, Phys. Rep., 568, 1.

[5] Koyama, K. 2016, Reports on Progress in Physics, 79, 046902.

[6] Li, B., & Koyama, K. 2019, Modified Gravity, World Scientific.

[7] Khoury, J., & Weltman, A. 2004, Phys. Rev. D, 69, 044026.

[8] Khoury, J., & Weltman, A. 2004, Phys. Rev. Lett., 93, 171104.

[9] Hinterbichler, K., & Khoury, J. 2010, Phys. Rev. Lett., 104, 231301.

[10] Brax, P., van de Bruck, C., Davis, A.-C., & Shaw, D. 2010, Phys. Rev. D, 82, 063519.

[11] Brax, P., Davis, A.-C., Li, B., & Winther, H. A. 2012, Phys. Rev. D, 86, 044015.

[12] Brax, P., et al. 2004, AIP conference proceedings, American Institute of Physics.

[13] Davis, A.-C., Lim, E. A., Sakstein, J., & Shaw, D. J. 2012, Phys. Rev. D, 85, 123006.

[14] Haghi, H., & Amiri, V. 2016, MNRAS, 463, 1944.

[15] Chang, P., & Hui, L. 2011, ApJ, 732, 25.

[16] Vikram, V., Sakstein, J., Davis, C., & Neil, A. 2018, Phys. Rev. D, 97, 104055.

[17] Desmond, H., Ferreira, P. G., Lavaux, G., & Jasche, J. 2019, MNRAS: Letters, 483, L64.

[18] Najafi, S., Mirtorabi, M. T., Ansari, Z., & Mota, D. F. 2019, J. Cosmology Astropart. Phys., 02, 011.

[19] Largani, N. K., & Mirtorabi, M. T. 2019, AIP Conf. Proc., 2163, 090008.

[20] Silvestri, A. 2011, Phys. Rev. Lett., 106, 251101.

[21] Sakstein, J. 2015. [arXiv:hep-ph/0108264]

[22] Burrage, C., & Sakstein, J. 2016, J. Cosmology Astropart. Phys., 2016, 045.

[23] Burrage, C., & Sakstein, J. 2018, Living reviews in relativity, 21, 1.

[24] Sakstein, J. 2018, International J. Modern Physics D, 27, 1848008.

[25] Brax, P., Casas, S., Desmond, H., & Elder, B. 2021, Universe, 8, 11.

[26] Baker, T., et al. 2021, Reviews of Modern Physics, 93, 015003.

[27] Jordi, K., et al. 2009, AJ, 137, 4586.

[28] Gentile, G., Famaey, B., Angus, G., & Kroupa, P. 2010, A&A, 509, A97.

[29] Sollima, A., & Nipoti, C. 2010, MNRAS, 401, 131.

[30] Ibata, R., et al. 2011, ApJ, 738, 186.

[31] Derakhshani, K., & Haghi, H. 2014, ApJ, 785, 166.

[32] Haghi, H., Baumgardt, H., & Kroupa, P. 2011, A&A, 527, A33.

[33] Hernandez, X., & Jiménez, M. 2012, ApJ, 750, 9.

[34] Moffat, J., & Toth, V. 2008, ApJ, 680, 1158.

[35] Llinares, C. 2018, MNRAS: Letters, 476, L29.

[36] Binney, J., & Tremaine, S. 1987, Galactic dynamics, Princeton University Press.

[37] King, I. R. 1966, ApJ, 71, 64.

[38] Waterhouse, T. P. 2006, An introduction to chameleon gravity. [arXiv:astro-ph/0611816]

[39] Bovy, J. 2017, Dynamics and Astrophysics of Galaxies, Princeton University Press, Princeton, NJ (in preparation).